

Expansion of research base/station in the Arctic

*Hiroyuki Enomoto¹

1. National Institute of Polar Research

Arctic Challenge for Sustainability (ArCS) project coordinate the use of Arctic stations, research sites and facilities for ArCS collaborators and also Japanese researchers.

The sites are, IARC (International Arctic Research Center)/UAF and Poker Flat observation site in US, CHARS (Canadian High Arctic Research Station) and CEN (Centre for Northern Studies) in Canada, observation sites in Cape Baranocva and Spasskaya Pad in Russia, Ny-Alesund and UNIS (The University Centre in Svalbard) in Svalbard, Norway, EGRIP (East Greenland Ice Coring Project) site and GINR (Greenland Institute of Natural Resources) at Nuuk, Greenland.

These sites and facilities are available for research and training of young scientists.

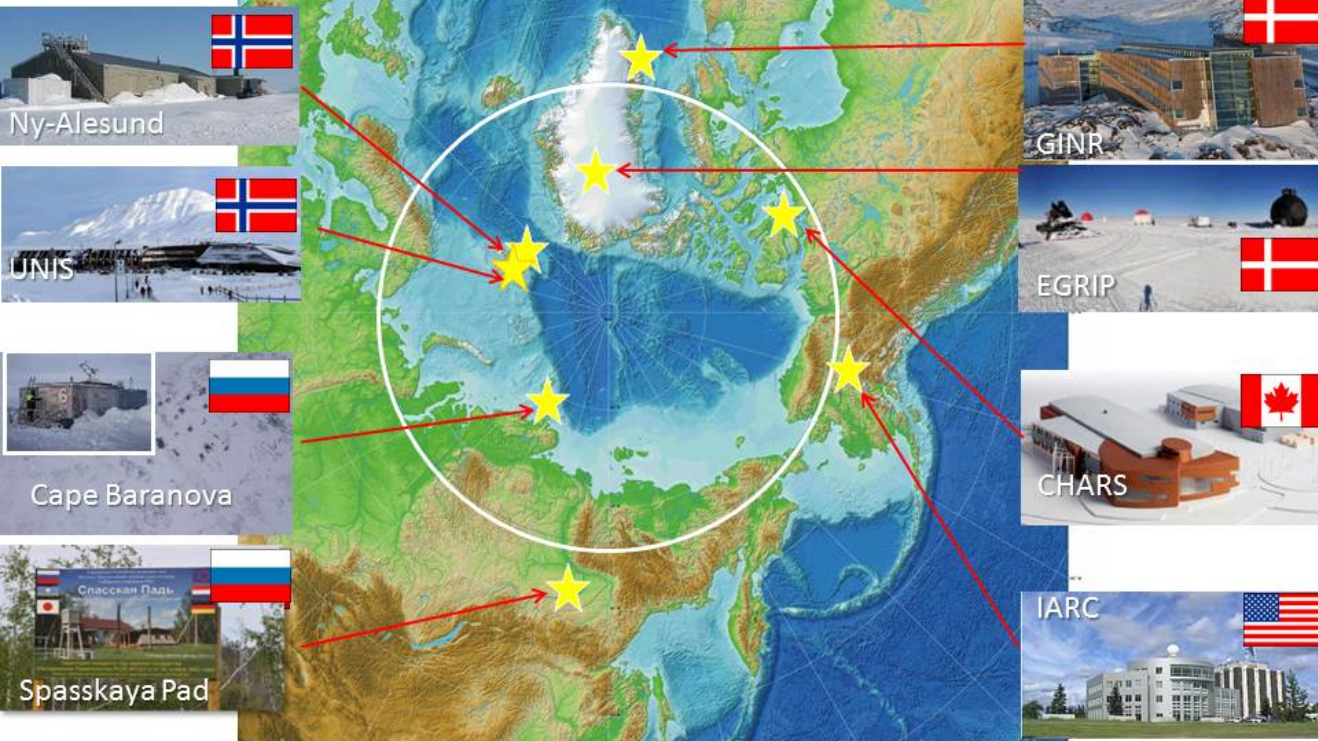
The presentaiton intoroduces the geographical distribution of pan-Arctic sites and their reseach targets, possible transfer to the social benefits, then discuss contribution to Japanese Arctic sciencific activities.

Keywords: Arctic, research sites, International scientific colaboration, international partnership



Japanese approach to the Arctic

Expand research base/collaborations



Improving the basic research facilities for long-term stay and/or monitoring studies, which can be used by international collaborative studies.

Water structures and circulation along with bio-geochemical processes in the Arctic Ocean suggested with nutrients and oxygen distributions

*Motoyoshi Ikeda^{1,2}, Shinichi Tanaka³, Yutaka Watanabe⁴

1. Hokkaido University, 2. JAMSTEC, 3. Earthquake Research Institute, The University of Tokyo, 4. Graduate School of Earth Environmental Science, Hokkaido University

Climatological water mass structures were identified in the Arctic Ocean, using the geochemical dataset in the Hydrochemical Atlas of the Arctic Ocean (HAAC). In addition, a geochemically conserved parameter PO_4^* was considered under the following process: when the water column remineralization of organic matter occurs, the content of phosphate increases with decline of dissolved oxygen according to remineralization stoichiometry at the rate of $P:O_2 = 1: -175$ (Anderson and Sarmiento, 1994). The equation is formulated as

$$PO_4^* = PO_4 + DO/175 - 1.95 \text{ (}\mu\text{ mol/L, Broecker, 1991)}$$

Once the values of PO_4^* are very close to each other, there is high possibility that they have a common origin.

In the upper ocean above 500-m depth, as widely known from various datasets, the Pacific-origin Water (P-Water) is clearly indicated with higher silicate, higher phosphate and lower dissolved oxygen than the Atlantic-origin Water (A-Water). The boundary between the water masses is located along 135°E-45°W at the surface and rotates counter-clockwise with depth, confirming the anti-cyclonic circulation of P-Water in the surface layer (0 to 200-m depth), and the cyclonic circulation of A-Water in the subsurface layer (200 to 500-m depth), exchanging between the Arctic and the Atlantic oceans, caused by the water density contrast. Therefore, the HAAC dataset is reliable as a supplier of oceanographic information for a half century.

In the lower ocean below 1500-m depth with the basins separated by the Lomonosov Ridge, dissolved oxygen is lower in the Canadian Basin than the Eurasian Basin. The lower phosphate and higher dissolved oxygen are limited to the vicinity of the Barents Sea and the Fram Strait. Useful information was obtained from PO_4^* (Table below): i.e., the lower-ocean water is maintained by a descending flow along the Siberian continental slope coming from the Atlantic through the Barents Sea, in addition to penetration of the Nordic Seas Deep Water flowing from the Greenland Sea. The former component circulates cyclonically to the Canadian Basin, as shown with $PO_4^* = 0.65 \sim 0.67$, along with the high core of $PO_4^* = 0.86$ at 2000m-depth in the southern Canada Basin under the influence of the shelf water. The latter component with $PO_4^* = 0.72$ spreads along the sea floor (3500-m depth) from the Atlantic side to the Pacific side.

The lower-ocean water mass gradually receives nutrients from sinking organic matters, and provides the intermediate-layer water between the upper and the lower oceans. The intermediate water is mostly occupied with A-Water and entrains water from the subsurface portion also, returning toward the Atlantic. Anderson and Sarmiento, 1994: *Global Biogeochemical Cycles*, **8**, 65-80.

Broecker, 1991: *Oceanography*, **4**, 79-89.

Table: The values of PO_4 and DO taken from the horizontal maps with rounding at 2%. The unit is $\mu\text{ mol/L}$. The values are confirmed with the vertical profiles.

Keywords: Arctic Ocean, geochemical tracer, remineralization, ocean circulation

Location	PO ₄	DO	PO ₄ *
Northern boundary of Barents Sea (200m & 500m)	0.85	310	0.67
Canadian Basin excluding high PO ₄ area (2000m) & all (2500m)	1.00	280	0.65
Canada Basin in high PO ₄ area (2000m)	1.15	290	0.86
Eurasian Basin (2000m & 2500m)	0.95	300	0.72
Greenland Sea Fram Strait (500m)	0.70	340	0.69
Greenland Sea Fram Strait (2000m)	0.70	310	0.52

Nutrient Dynamics Affecting Phytoplankton Distributions in the Pacific Arctic Region

*Shigeto Nishino¹, Takashi Kikuchi¹, Michiyo Yamamoto-kawai², Yusuke Kawaguchi¹, Toru Hirawake³, Motoyo Itoh¹, Amane Fujiwara¹, Michio Aoyama^{4,1}

1. JAMSTEC Japan Agency for Marine-Earth Science and Technology, 2. Tokyo University of Marine Science and Technology, 3. Hokkaido University, 4. Fukushima University

The Chukchi Sea and Canada Basin are areas in the Pacific Arctic characterized by northward advection and spreading of Pacific-origin water that transports nutrients into the Arctic Ocean, and thus plays an important role in phytoplankton distributions. In this study, we examined ship-based and mooring data to understand nutrient dynamics and its influence on phytoplankton distributions. In the southern Chukchi Sea, our data suggest that, in contrast to spring blooms that are caused by a nutrient supply with the advection of Pacific-origin water, autumn blooms there are maintained by regenerated nutrients from the bottom of the shallow sea where particulate organic matters are largely accumulated in autumn. On the other hand, large-scale ocean circulation controls nutrient distributions in the Canada Basin where sea ice reduction in recent years has changed the ocean circulation and thus impacts on the nutrient and phytoplankton dynamics. We found that oceanographic and biological responses to the sea ice loss are quite different between the Alaskan and Siberian sides of the region. On the Alaskan side, eddies also play an important role in the nutrient and phytoplankton distributions. However, on the Siberian side, data are still lacking and various biogeochemical processes should be clarified in future studies.

Keywords: Arctic Ocean, Sea ice reduction, Ocean circulation, Eddy, Nutrients, Phytoplankton

Species invasion and diversity in benthic macrofaunal communities in the Pacific Arctic

*Hisatomo Waga¹, Toru Hirawake², Jacqueline M Grebmeier³

1. Graduate School of Fisheries Sciences, Hokkaido University, 2. Faculty of Fisheries Sciences, Hokkaido University, 3. Chesapeake Biological Laboratory, University of Maryland Center for Environmental Science

There is growing evidence of increased Pacific water transport into the Arctic that is influenced by variations in atmospheric forcing. One of the empirical and theoretical predictions for a future Arctic impacted by increased Pacific water transport is that new taxa will expand or invade the Arctic ecosystem. However, well-documented examples are still scarce due to the limited number of time-series measurements in the Arctic, particularly for benthic organisms. Although benthic organisms are normally stationary and less mobile than fishes, seabirds and mammals, it seems relevant that benthic organisms with pelagic life stages will be less limited in their expansion abilities. In this study, the relationship between the number of benthic macrofaunal taxa and atmospheric forcing was investigated in the Pacific Arctic. Average taxon number of benthic macrofauna for 2010–2012 has increased significantly compared to 2000–2006 on the continental shelf area from south of St. Lawrence Island in the northern Bering Sea to just north of St. Lawrence Island in the Chirikov Basin, likely caused by the difference in magnitude and location of the Aleutian Low. By comparison, the biomass-based Shannon-Weaver diversity index did not reflect the changes in taxon number of benthic macrofauna. These results indicate increased invasion of new taxa into the region for 2010–2012 compared to 2000–2006, but the biomass of new taxa is negligible when compared with the total benthic macrofaunal biomass. Our findings demonstrated indications of ongoing changes that could continually be facilitated by climate change to future Arctic marine ecosystems in the Pacific Arctic region.

Keywords: Arctic, Benthic community, Pacific water transport

Evaluation of riverine heat inflow in the Arctic Ocean modeling

*Eiji Watanabe¹, Hotaek Park¹, Tatsuo Suzuki¹, Dai Yamazaki¹

1. Japan Agency for Marine-Earth Science and Technology: JAMSTEC

River water is known as important sources of freshwater and nutrients in the Arctic Ocean. Its spatial distribution has been widely visualized using observed chemical properties and numerical tracer experiments. However, continuous monitoring of the volume flux is limited only at major river stations. A substantial amount of uncertainties still remains particularly on ungauged rivers. We compared a couple of river water discharge datasets in the Arctic Ocean modeling. The Arctic Ocean Model Intercomparison Project (AOMIP) traditionally adopted monthly climatology of 13 major rivers, which was based on the R-ArcticNET data archive. The ungauged inflow was added under simple assumption. A daily discharge dataset covering most Arctic sea coasts and multiple decades was recently developed by combining land runoff of the Japanese 55-year reanalysis for driving ocean and sea ice models (JRA55-do) and drainage of the Catchment-based macro-scale floodplain scheme (CaMa-Flood). Another daily discharge dataset was provided using the coupled hydrological and biogeochemical model (CHANGE) and the Total Runoff Integrating Pathways scheme version 2 (TRIP2). An originality of the third dataset is explicit calculation of river ice and snow loading so that the gridded data of river water temperature are also available. In this study, to evaluate an impact of riverine heat inflow on sea ice in the Arctic Ocean, decadal experiments for 1979–2013 were performed using the Center for Climate System Research Ocean Component model version 4.9 (COCO4.9) in the pan-Arctic regional framework. The horizontal grid size was set to approximately 25 km, and atmospheric forcing components were constructed from the National Centers for Environmental Prediction–Climate Forecast System Reanalysis (NCEP–CFRS). First, the riverine volume inflow was given by three datasets, respectively, so that the sensitivity of sea ice and hydrography was checked. The model results in these cases showed similar interannual variability of sea ice thickness and sea surface salinity in each sub-domain (e.g., Kara and Beaufort seas). We then incorporated the river water temperature into the model experiment. The annual mean sea ice thickness in this case produced negative anomaly over the Siberian shelves and in the southern Canada Basin. The seasonal transitions in sea ice concentration and sea surface temperature indicated that riverine heat inflow into the Arctic Ocean accelerated summer sea ice opening and sea surface warming in the vicinity of major river mouths.

Keywords: Arctic Ocean model, land–ocean interaction, river water temperature, sea ice melting

Variability of sea-ice thickness in the northeastern coastal Chukchi Sea revealed by a moored ice-profiling sonar

*Yasushi Fukamachi¹, Daisuke Simizu², Kay I. Ohshima¹, Hajo Eicken³, Andrew R. Mahoney³, Katsushi Iwamoto⁴, Erika Moriya⁵, Sohey Nihashi⁶

1. Hokkaido University, 2. National Institute of Polar Research, 3. University of Alaska Fairbanks, 4. City of Mombetsu, 5. Hydro Systems Development, Inc., 6. National Institute of Technology, Tomakomai College

Using a moored ice-profiling sonar, time-series ice-draft data were obtained in a coastal region of the northeastern Chukchi Sea during 2009-10 for the first time. Time-series data show seasonal growth of sea-ice draft, which is occasionally interrupted by the appearances of coastal polynya and upwelled Atlantic Water. The sea-ice draft distribution indicates the abundance of thicker ice comparable or less than in the adjacent Beaufort Sea. The rapid increase of thicker ice from December to January corresponded to the minimal offshore drift in January and the resulting rapid decrease of level-ice fraction indicating dynamical thickening processes. The mean draft and its converted thickness are 1.27 and 1.54 m, respectively. Heat losses are calculated with ice-thickness data averaged over various time scales corresponding to various spatial scales. Comparing to the estimate with ice-thickness data every second, these estimates are roughly two thirds and a half for the cases with spatial averaging over ~20 and 100 km, respectively. The heat-loss estimate based on thin-ice data derived from the AMSR-E corresponds well with the estimate based on the 1-second observed ice-thickness data, indicating the validity of a thin-ice thickness algorithm and the resulting heat-loss estimate based on the AMSR-E data.

Keywords: sea-ice thickness, Chukchi Sea, ice-profiling sonar

Can the anticyclonic eddy trap and amplify near-inertial waves in the Arctic Ocean?

*Eun Yae Son¹, Yusuke Kawaguchi², Jae-Hun Park¹, Ho Kyung Ha¹

1. Inha University, 2. JAMSTEC

The hydrographic data obtained by the Ice-Tethered Profiler with Velocity (ITP-V) were utilized to reveal the eddy-internal wave interaction in the Canada Basin, Arctic. The ITP-V is an autonomous drifting instrument that collects profiles of hydrographic data and velocity concurrently in depths of 10-250 m at 3-hr interval. The observation using the ITP-V, installed on the multi-year sea ice, was operated for 9 months from August 2014. We focus on a specific event in mid-October, when a near-surface anticyclonic eddy was observed in depths of 50-100 m. The anticyclonic eddy showed vertically stretched isopycnals with anomalously warm water in its core. It is noted that the near-inertial internal waves were trapped and amplified near the bottom of the eddy, where the horizontal and vertical wave lengths were approximately 10 km and 60 m, respectively. The parameterized turbulent diffusivity (Gregg, 1989) reached up to $10^{-5} \text{ m}^2/\text{s}$ near the bottom of the eddy while the background diffusivity was around $10^{-7} \text{ m}^2/\text{s}$. Our results demonstrate that near-inertial waves can be trapped and amplified within the anticyclonic eddy in the Arctic and can enhance the ocean mixing like mid latitudes.

Keywords: Near-inertial internal waves, anticyclonic eddy, fine-scale parameterization, Canada Basin

Interannual salinity variations in the northwestern Bering Sea associated with the Bering Strait throughflow

*Yoshimi Kawai¹, Satoshi Osafune¹, Shuhei Masuda¹, Yoshiki Komuro²

1. Research and Development Center for Global Change, Japan Agency for Marine-Earth Science and Technology, 2. Institute of Arctic Climate and Environment Research, Japan Agency for Marine-Earth Science and Technology

The relationship between the Bering Strait throughflow (BTF) and sea surface salinity (SSS) in the Bering Sea was investigated mainly using an atmosphere-ocean-ice coupled model, MIROC4h, which includes an eddy-permitting ocean model. The MIROC4h simulated well the seasonal cycle of BTF transport, although it overestimated the transport compared with mooring-based estimates. The interannual variations of SSS in the Bering Sea were correlated with those of BTF transport: SSS in the northwestern Bering Sea was high when BTF transport was large. And there was seasonality in the relationship between SSS and BTF. The SSS anomaly associated with the BTF anomaly became evident from winter to spring, and SSS lagged behind the BTF by a few months. Similar relationship between the BTF and SSS can be seen in an observation dataset and two kinds of ocean data assimilation product, although there were some differences from the MIROC4h in the spatial distribution and the timing of large r . Sea surface temperature (SST) also became higher with the larger BTF transport in the cold season, however, the surface density were affected by the SSS anomalies more than the SST ones. BTF transport was strongly correlated with SSH in the eastern Bering Sea, the southwestern Chukchi Sea (CS), and the East Siberian Sea (ESS); there was no time lag between the BTF and SSH. The low SSH along the Siberian coast was uncorrelated with the high SSH in the Bering Sea. The Arctic SSH affected BTF transport and the SSS in the northwestern Bering Sea independently of the SSH in the Bering Sea. The r between the SSH and zonal wind stress suggested that shelf waves might be excited by zonal wind anomalies in the Laptev Sea or north of the New Siberian Islands to propagate to the Bering Strait. The low SSH along the Siberian coast associated with high SSS in the northwestern Bering Sea, however, was not confirmed in 10 years of satellite-derived SSH data. The relationship between the Arctic SSH and SSS in the Bering Sea still needs to be further investigated.

We evaluated the salt budget in the northwestern Bering Sea using the MIROC4h data. When the BTF transport in October–March was large, the horizontal salt advection increased and meltwater decreased; both changes contributed to the mixed-layer salinization, but the horizontal advection term dominated north of 62.5°N, and the sea-ice melting term did south of 62.5°N. The residual term, which mainly represented eddy diffusion, had a role to suppress the magnitude of the salinity tendency. The same features can be seen when the SSH in the southwestern CS and the ESS was low in the cold season. In these cases, the near-surface current anomalies across the contours of salinity were reinforced, and the horizontal salt convergence occurred in the northwestern part of the Bering Sea. Furthermore, the anomalous southerlies and currents contributed to the sea-ice retreat. The SSH anomalies in the Arctic Ocean affected the currents in Bering Strait and the northwestern Bering Sea, perhaps through the propagation of shelf waves, to lead to the salinization. The current anomalies in the northwestern part associated with the BTF or SSH anomalies became weaker in the warm season, which produced the seasonality of the correlation.

Keywords: Bering Strait throughflow, sea surface salinity, sea surface height, MIROC4h

Subglacial meltwater discharge and its impact on water properties in Bowdoin Fjord, northwestern Greenland

*Yoshihiko Ohashi^{1,2}, Shigeru Aoki², Yoshimasa Matsumura², Shin Sugiyama^{2,3}, Naoya Kanna³, Daiki Sakakibara³, Yasushi Fukamachi^{2,3}

1. Graduate School of Environmental Science, Hokkaido University, 2. Institute of Low Temperature Science, Hokkaido University, 3. Arctic Research Center, Hokkaido University

Meltwater runoff from the Greenland ice sheet to the ocean has increased in recent years. Thus, it is important to assess the impact of meltwater runoff on the oceanic structure. In marine-terminating glaciers, subglacial meltwater discharge occurs at the grounding line depth and forms an upwelling plume. To understand the impact of subglacial meltwater discharge on water properties, we carried out CTD observations in Bowdoin Fjord, northwestern Greenland in the summers of 2014 and 2016. A numerical experiment of subglacial meltwater plume was also performed with a non-hydrostatic ocean model to examine the effects of freshwater flux changes.

In ocean observations of 2014 and 2016, a significantly high turbidity layer (> 5 FTU) was observed at the subsurface of 20–40 m depth, which was caused by subglacial meltwater plume. Moreover, the level of turbidity and potential temperature showed interannual variations: turbidity was higher and temperature was lower near the surface (5–15 m depth) in 2016, whereas turbidity was lower and temperature was higher at the layer below (50–100 m depth). The observed structure suggests that a larger discharge of turbid subglacial meltwater in 2016, with a larger buoyant force, mixed with the fjord water at the grounding line depth and extended at the relatively shallower depths. The situation is consistent with the fact that the sum of positive degree days at Qaanaaq Airport, a proxy for meltwater runoff in this region, was approximately 20% greater in 2016 than in 2014. In the numerical experiment with 20% greater amount of freshwater flux, concentration of a meltwater tracer near the surface increased by roughly 20% from that of the control case, whereas the tracer concentration decreased at the layer below. The difference in the vertical distribution of tracer concentration with and without increasing the freshwater flux was consistent with that of turbidity in the two years. These results indicate that the change in amount of subglacial meltwater runoff affects the behavior of turbid subglacial meltwater plume and material transport, which might further impact on biogeochemical cycles.

Keywords: Glacier-ocean interaction, Subglacial meltwater plume, Water properties, Fjord, Greenland

Characterizing landscape-scale distribution of sparse larch forest and surrounding wetland in Taiga-Tundra boundary ecosystem, Northeastern Siberia

*Tomoki Morozumi¹, Atsuko Sugimoto^{2,1}, Ryo Shingubara¹, Shinya Takano¹, Ruslan Shakhmatov¹, Rong Fan¹, Shunsuke Tei², Hideki Kobayashi³, Rikie Suzuki³, Trofim C Maximov^{4,5}

1. Graduate School of Environmental Science, Hokkaido University, 2. Arctic Research Center, Hokkaido University, 3. Department of environmental geochemical cycle research, JAMSTEC, 4. Institute for Biological Problems of Cryolithozone SB RAS, 5. BEST center, North Eastern Federal University

Vegetation cover is essential information for upscaling GHG emission in local to regional scale. Taiga-Tundra boundary ecosystem consists of sparse Larch forest and polygonal wetland in eastern Siberia, and it is no easy task to know the structure of heterogeneous landscape. Field observation and high resolution satellite image provide information for vegetation cover on a microtopographic level, while coarser resolution image contains mixed pixels. To evaluate fraction of small vegetation patch, subpixel classification has been applied at coarser resolution satellite image. In this study ALOS AVNIR2 (JAXA) reflectance image (70 x 70 km) was classified into landscape unit and then subpixel vegetation cover was obtained by linear spectral unmixing (LSU) method based on vegetation endmember of field reflectance and tree distribution survey in Indigirka lowland eastern Siberia (70°N, 148°E) in July summer. Result was validated by higher resolution vegetation map that was derived from WorldView-2 (Digital Globe) for 10 x 10 km.

AVNIR2 image was classified into 15 landscape units by ISODATA unsupervised classification. Each landscape unit in 10m resolution AVNIR2 image contained usually 2 to 4 dominated vegetation classes in 2-0.5 resolution WorldView-2 vegetation map. For example, a landscape unit near tributary consisted of Sedge, Shrub and smaller fraction such as Tree and Salix endmembers. After endmember collection, subpixel vegetation cover was estimated for 70 x 70km scale, and it revealed landscape-scale distribution and zonation of vegetation cover in Taiga-Tundra boundary. Prior to this study, we have investigated CH₄ emission and biomass production of willow bush for 10 x 10km local scale in this observation area. This subpixel vegetation data will allow us to upscale these parameters on biogeochemical cycles for larger spatial scale.

Keywords: vegetation, landscape, subpixel classification

Highly Dynamic Methane Emission from the West Siberian Boreal Floodplains

Irina Terentieva, Alexander Sabrekov^{1,2}, Ali Ebrahimi³, Mikhail Glagolev^{1,2,4,5}, *Shamil S Maksyutov⁶

1. Tomsk State University, 36 Lenina Street, Tomsk 643050, Russia, 2. Institute of Forest Science, Russian Academy of Sciences, 21 Sovetskaya st., Uspenskoe, Moscow region 143030, Russia, 3. Department of Environmental Systems Science, ETH Zurich, 8092 Zurich, Switzerland, 4. Yugra State University, 16 Chekhova st., Khanty-Mansiysk 628012, Russia, 5. Moscow State University, 1 Leninskie gory, Moscow 119992, Russia, 6. National Institute for Environmental Studies, 16-2 Onogawa, Tsukuba, Ibaraki, 305-8506, Japan

Methane production from riparian wetlands may cause significant CH₄ emissions to the atmosphere. However, seasonal floodplains of many high-latitude rivers are still not represented in studies on methane emissions. A major river in West Siberia is Ob River; it is one of the longest rivers in the world. Despite its potential importance, field observations of the CH₄ fluxes in that domain were mainly focused on peatlands and lakes. The present study is a first attempt to estimate variability of methane fluxes from West Siberian boreal floodplains. Results of the study can be used for further data upscaling, especially in combination with floodplain area data.

Methane emission measurements were made by static chamber method during 2015-16 summer periods. Test sites were located at the Ob River floodplain near Khanty-Mansiysk city, Russia, as well as within smaller floodplains in taiga zone.

Flux medians varied in two orders of magnitude from zero to 17.5 mgC/m²/h. Aiming at further upscaling, we managed such heterogeneity by classifying studied environments with following criteria: i) floodplain width (small or large), ii) microrelief (elevated or depressed), iii) inundation during the measurements («wet» or «dry»). Within this framework, several classes were found to be similar in CH₄ emission rates: i) «wet» and «dry» depressions of large floodplains had highest fluxes of 4.21 mgC/m²/h with interquartile range (IQR) of 5.17 mgC/m²/h, ii) «wet» elevations within large floodplains and all small «wet» floodplains had lower flux median of 1.47 mgC/m²/h with IQR of 2.99 mgC/m²/h, iii) «dry» elevations within large floodplains and all small «dry» floodplains had the lowest median of 0.07 mgC/m²/h with IQR of 0.26 mgC/m²/h.

This observations highlight high variability of emission, which is most evident in depressions within large floodplains, where a few rare but large emission events can contribute significantly to the total emission rates. It was also found that there were only slight difference between emissions from «wet» and «dry» depressions. It can be related to the presence of constant overwetting due to close position of underground waters or water accumulation after precipitation periods.

Besides the common variability of methane fluxes, we also observed «hot moments» of methane emission. In particular, time-series measurements at Ob floodplain revealed sudden peak in emissions just after the main water subsiding (comparing to the fluxes during the flooding period). Results also indicated gradual decreasing of emissions and its dispersion from 5.89 mgC/m²/h to 3.51 mgC/m²/h during two weeks of soil drying. We hypothesize that gas bubbles were initially accumulated in soil during the inundated period when the gas diffusion rate was limited and hydrostatic pressure was high. Such accumulation was confirmed by dissolved CH₄ concentration measurements in sediments revealing 10 times higher CH₄ concentration in comparison with the water column. We suggested that further methane release could be triggered by abrupt hydrostatic pressure decrease induced by water drawdown. Since the threshold concentration of dissolved methane correlates with the water column depth, water level drop might lead to gas generation from the solution and the enlargement of the volume of the gas phase with further

ebullition.

As the next step, we need systematic measurements of methane fluxes and their combining with floodplain mapping for further data upscaling.

Keywords: wetlands, methane, greenhouse gasses, arctic, Siberia

Assessing and projecting greenhouse gas release from dynamic permafrost degradation

*Kazuyuki Saito¹, Hiroshi Ohno², Tokuta Yokohata³, Go Iwahana⁴, Hirokazu Machiya¹

1. Japan Agency for Marine-Earth Science and Technology, 2. Kitami Institute of Technology, 3. National Institute for Environmental Studies, 4. University of Alaska Fairbanks

Permafrost is a large reservoir of frozen soil organic carbon (SOC; about half of all the terrestrial storage). Therefore, its degradation (i.e., thawing) under global warming may lead to a substantial amount of additional greenhouse gas (GHG) release. However, understanding of the processes, geographical distribution of such hazards, and implementation of the relevant processes in the advanced climate models are insufficient yet so that variations in permafrost remains one of the large source of uncertainty in climatic and biogeochemical assessment and projections. Thermokarst, induced by melting of ground ice in ice-rich permafrost, leads to dynamic surface subsidence up to 60 m, which further affects local and regional societies and eco-systems in the Arctic. It can also accelerate a large-scale warming process through a positive feedback between released GHGs (especially methane), atmospheric warming and permafrost degradation. This three-year research project (2-1605, Environment Research and Technology Development Fund of the Ministry of the Environment, Japan) aims to assess and project the impacts of GHG release through dynamic permafrost degradation through in-situ and remote (e.g., satellite and airborne) observations, lab analysis of sampled ice and soil cores, and numerical modeling, by demonstrating the vulnerability distribution and relative impacts between large-scale degradation and such dynamic degradation. Our preliminary laboratory analysis of ice and soil cores sampled in 2016 at the Alaskan and Siberian sites largely underlain by ice-rich permafrost, shows that, although gas volumes trapped in unit mass are more or less homogenous among sites both for ice and soil cores, large variations are found in the methane concentration in the trapped gases, ranging from a few ppm (similar to that of the atmosphere) to hundreds of thousands ppm. We will also present our numerical approach to evaluate relative impacts of GHGs released through dynamic permafrost degradations, by implementing conceptual modeling to assess and project distribution and affected amount of ground ice and SOC.

Keywords: Ice-rich permafrost degradation, Methane, climate change, tipping point

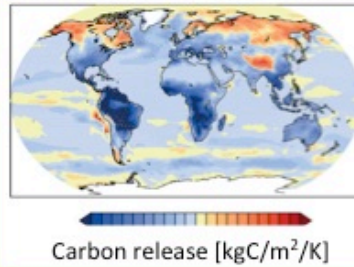
Assessing and projecting greenhouse gas release from dynamic permafrost degradation

【ERTDF 2-1605 FY2016-18】



Model improvement, Projections

- Quantification of potential methane release
- Refined future climate projections etc.

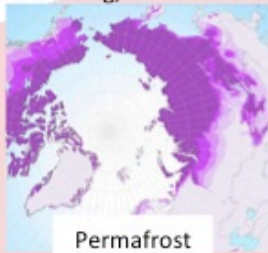


Previous studies
Incremental and kinetic degradation
→ Need to incorporate local but dynamic degradation

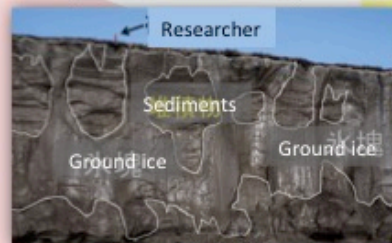
Sub theme 3:

Projecting future gas release by integrated land surface model with explicit permafrost dynamics (NIES)

Understanding of vulnerability
(remote-sensing, numerical modeling)



Ice-rich permafrost



Sampling and lab-analyses of methane in ice cores



Sub theme 1:

Assessing dynamic permafrost degradation mechanism and vulnerability (JAMSTEC)

Sub theme 2:

Quantifying organic carbon content (GHG) in large permafrost ice and sediments (Kitami Inst. of Technology)

Impact of Arctic sea ice decline on recently observed climate change: a coordinated multi-model study

*Noel S Keenlyside^{1,2,3}, Fumiaki Ogawa^{1,3}, HoNam Hoffman Cheung^{1,3}, Yongqi Gao^{2,3,1}, Torben Koenigk⁴, Vladimir Semenov⁵, Lingling Suo^{2,3}, Shuting Yang⁶, Tao Wang⁷, Martin Peter King^{8,3}, Guillaume Gastineau⁹, Sergey Gulev¹⁰

1. Geophysical Institute, University of Bergen, 2. Nansen Environmental and Remote Sensing Center, 3. Bjerknes Centre for Climate Research, 4. Swedish Meteorological and Hydrological Institute, Sweden, 5. Helmholtz centre for ocean research Kiel GEOMAR, Germany, 6. Danish Meteorological Institute, Denmark, 7. Institute of Atmospheric Physics, China, 8. Uni-Research Climate, Norway, 9. Sorbonne universities, France, 10. Shirshov Institute of Oceanology, Russia

To what extent the recent sea-ice decline influenced Northern Hemisphere climate trends remains an open question. To address this we perform two atmospheric general circulation model experiments: In both experiments observed daily sea ice cover variations are prescribed for the period 1982 to present, while for SST, one experiment uses observed daily variations and the other the observed climatology. The experiment is performed by six different state-of-the-art AGCMs. Our results show that the observed wintertime temperature trend near the surface is poorly reproduced. The impact of SIC variation seems to be confined near the surface, while SST variation seems a key for temperature trend above. This suggests a necessity to consider the atmospheric poleward energy transport associated with SST variation to understand the observed arctic amplification. The simulations fail to reproduce the observed changes in the Siberian High and Eurasian wintertime cooling. Northern hemisphere surface and zonal mean tropospheric temperature trends are better reproduced in boreal autumn, but the impact of sea ice decline remains limited to the lower troposphere. Other aspects of SIC/SST impact on the observed circulation change such as NAO shall also be discussed.

Keywords: Sea ice decline, Climate Change, Sea ice impact

Evaluation of Atmospheric Response to Arctic Sea Ice Anomalies

*Masato Mori¹

1. Research Center for Advanced Science and Technology, the University of Tokyo

During the last decade, severe winters occurred frequently in mid-latitude Eurasia, despite increasing global- and annual-mean surface air temperature. Statistical analyses of observational data have suggested that some part of these cold winters were forced by Arctic sea-ice decline. However, numerical modelling studies have shown different conclusion depending on the used model and experimental settings, and whether or not the cause is due to sea ice reduction is controversial. Therefore, it is important to clarify the cause of the diversity of simulation results, especially the extent to which sea ice anomaly controls the atmospheric circulation.

In this research, we successfully detected the signature of Eurasian cold winters excited by sea-ice decline in the Barents-Kara Sea, by generating a four kind of long-term historical and large-member ensemble simulation based on atmospheric general circulation model (AGCM). The sea ice reduction tends to increase occurrence frequency of cold winter over the central Eurasia, but its effect may have been underestimated in the AGCM. We conclude that this is one of the big reasons that conclusion change depending on model experiments.

Keywords: sea ice, the Arctic, cold winter

Baroclinic Wave Response to the Arctic Amplification of Global Warming

*Hiroshi Tanaka¹, Makoto Sakurai²

1. Center for Computational Sciences, University of Tsukuba, 2. School of Life and Environmental Science, University of Tsukuba

The Arctic warms twice faster than the global average of the warming trends. This response to the global warming is called Arctic Amplification (AA). Pronounced AA occurs in fall to winter seasons due to the ice-albedo feedback, cloud feedback, and the enhanced meridional heat and moisture transports. The meridional transports are accompanied by baroclinic waves in mid-latitudes, and the transports are expected to decrease by the AA owing to the reduced baroclinicity. The purpose of this study is to investigate the changing baroclinic instability in response to the AA by means of the theoretical linear stability analysis. According to the result of the analysis, the growth rate of the baroclinic waves decreases by the AA. The structure of baroclinic waves changes so as to reduce the eddy momentum transport to the polar jet in high latitudes. It is found that a positive feedback exists between the weaker polar jet and reduced eddy momentum transport to the jet in association with the AA.

Keywords: Arctic amplification, Baroclinic instability waves, Linear stability analysis, Baroclinic eddies, Eddy momentum transport

Interannual variation of snow grain size on Greenland ice sheet retrieved from MODIS data –difference between Terra, Aqua and their composite –

*Teruo Aoki^{1,2}, Rigen Shimada³, Tomonori Tanikawa², Masashi Niwano², Hiroshi Ishimoto², Masahiro Hori³, Knut Stamnes⁴, Wei Li⁴, Nan Chen⁴

1. The Graduate School of Natural Science and Technology, Okayama University, 2. Meteorological Research Institute, Japan Meteorological Agency, 3. Earth Observation Research Center, Japan Aerospace Exploration Agency, 4. Department of Physics and Engineering Physics, Steven Institute of Technology

Surface albedo in accumulation area of Greenland ice (GrIS) sheet mainly controlled by variation of snow grain size because snow impurity concentration is low. Recent warming in the Arctic could accelerate snow metamorphism and thus bring snow grain growth. Possible cause of recent darkening in accumulation area of GrIS is snow grain growth, which has a positive feedback to the further warming in the Arctic. Satellite remote sensing is an efficient tool for monitoring of snow parameters. However, long-term variation of satellite sensor sensitivity may affect the retrieval result of grain size as well. MODIS onboard Terra and Aqua is one of the most suitable satellite sensors to retrieve snow grain size, but it is reported that the sensor degradation of Terra/MODIS is more significant than Aqua/MODIS (Polashenski et al., 2015). Hence, it could affect the long-term variation of snow grain size retrieved. Recently, sensor sensitivity-corrected data set of Terra and Aqua/MODIS (C6) were released (Lyapustin et al., 2014). Using these data, we retrieved surface snow grain size (Rs1) on GrIS from Terra and Aqua independently, with the algorithm based on a look-up table (LUT) method (Stamnes et al., 2007) at the wavelength of 1.24 μ m. The LUT for bidirectional reflectance distribution function was calculated with a radiative transfer model for the atmosphere-snow system (Aoki et al., 2000) using a snow shape model employing Voronoi columns and aggregates (Ishimoto et al., 2012).

To analyze long-term variation of Rs1, monthly mean for all snow-covered area in GrIS was calculated from monthly mean image of Rs1, which is calculated from the daily images of Rs1 on GrIS. Comparing monthly mean Rs1 between Terra and Aqua, the monthly mean values of Rs1 derived from Terra were slightly smaller than those from Aqua. The differences are almost less than 10%. Since the year of launch differs between Terra and Aqua, we compared the interannual trend of Rs1 during the same period from 2003 to 2016 for Terra and Aqua. Both interannual trends from April to September agree well each other. Then, we calculated composite Rs1 from Terra and Aqua, by which we investigated variation of Rs1 for 2000-2016. The result shows that interannual trend of Rs1 is the largest (+32 μ m/decade) in July and small positive in April, May, June and August, and negative in September. However, this situation changes for plateau area higher than 3 km, for which the largest interannual trend of Rs1 is relatively small (+14 μ m/decade) in July and furthermore small positive in April, May, June and August, and small negative in September. These results mean the snow surface grain size on GrIS has an increasing trend except for September during 2000-2016 and thus contributes to albedo reduction.

References

- Aoki et al., 2000: *J. Geophys. Res.*, **105**, 10219-10236, doi:10.1029/1999JD901122.
Ishimoto et al., 2012: *J. Quant. Spectrosc. Radiat. Transfer*, **113**, 632-643, doi:10.1016/j.jqsrt.2012.01.017.
Lyapustin et al., 2014, *Atmos. Meas. Tech.*, **7**, 4353-4365, doi:10.5194/amt-7-4353-2014.

Polashenski et al., 2015, *Geophys. Res. Lett.*, **42**, doi:10.1002/2015GL065912.

Stamnes et al., 2007, *Remote Sens. Environ.*, **111**, 258-273, doi:10.1016/j.rse.2007.03.023.

Keywords: snow grain size, albedo, Greenland ice sheet, satellite remote sensing, MODIS

Variations in Sr and Nd isotopic ratios of mineral particles in cryoconite in western Greenland

*Naoko Nagatsuka¹, Nozomu Takeuchi², Jun Uetake¹, Rigen Shimada³, Yukihiro Onuma⁴, Sota Tanaka², Takanori Nakano⁵

1. National Institute of Polar Research, 2. Chiba University, 3. JAXA, 4. University of Tokyo, 5. Waseda University

Recently, the area of dark-colored ice has expanded and reduced surface albedo on the Greenland Ice Sheet. One of the possible causes of dark ice expansion is an increase in cryoconite, which is a dark colored surface dust consisting of mineral particles and organic matters. In order to better understand the source and transportation process of minerals on the dark-colored ice, we analyzed the Sr and Nd isotopic ratios of minerals in cryoconite, which were collected from glaciers in northwest and southwest Greenland.

The mineral components of the cryoconite showed variable Sr and Nd isotopic ratios, which corresponded to those of the englacial dust and moraine on and around the glaciers but were significantly different from those of the distant deserts that have been considered to be primary sources of mineral dust on the Greenland Ice Sheet. This suggests that the minerals within the cryoconites were mainly derived from local sediments, rather than from distant areas. The Sr ratios in the northwestern region were significantly higher than those in the southwestern region. This is probably due to geological differences in the source areas, such as the surrounding glaciers in each region.

The isotopic ratios further varied spatially within a glacier (Qaanaaq and Kangerlussuaq areas), indicating that the minerals on the glaciers were derived not from a single source but from multiple sources, such as englacial dust and wind-blown minerals from the moraine surrounding the glaciers.

Keywords: Greenland, Darkening of glaciers, Sr and Nd isotopic ratios, Mineral source

Meltwater floods at Qaanaaq ice cap in northwestern Greenland investigated by using a surface mass balance model

*Daiki Sakakibara^{1,2}, Masashi Niwano³, Shin Sugiyama²

1. Arctic Research Center, Hokkaido University, 2. Institute of Low Temperature Science, Hokkaido University, 3. Physical Meteorology Research Department, Meteorological Research Institute

Melt increase in the Greenland ice sheet and peripheral ice caps give impact on coastal environment, but only a few studies have focused on its influence on the human activity in Greenland. Qaanaaq, a village in northwestern Greenland populated by 500 people, has been a base for field campaigns conducted by the GRENE and ArCS projects. On 21 July 2015 and 3 August 2016, streams flooded in the village, which resulted in destruction of a road between the village and Qaanaaq Airport. These floods were caused by increased runoff from Qaanaaq ice cap located several kilometers from the village. Similar floods were recorded in the past, but the one in 2016 caused unusually serious damage. Possibly, these floods are the results of recently changing climatic conditions in the Arctic region.

In this study, we investigated the floods in 2015 and 2016 by using a surface mass balance model NHM-SMAP (Niwano *et al.*, 2012, 2014). Model output at 5 km mesh grid points was downscaled to a 300 m grid, using the method proposed by Noël *et al.* (2016). This method considers the dependence of snow and ice melt rate on elevation. Digital elevation model and ice mask provided by Byrd Polar and Climate Research Center were used for this procedure (Howat *et al.*, 2014). We compared downscaled surface mass balance with the observational data acquired in 2012–2016. Then we estimated the amount of runoff from Qaanaaq ice cap.

Runoff from Qaanaaq ice cap was significantly larger than usual on 21 July 2015 and 2 August 2016, the day and the previous day of the flood in 2015 and 2016, respectively. The runoff computed for 21 July was the second greatest in 2015. Daily mean air temperature observed at Qaanaaq airport showed the highest in the year during the period from 21 to 23 July. In the upper part of the ice cap, the largest amount of melting in the year was calculated on the day of the flood. No significantly large melting was computed after the flood in 2015. Runoff on 2 August was the third largest in 2016, which corresponds to the largest amount of daily rainfall. From these results, rapid melting and strong rainfall were suggested as the causes of the floods in 2015 and 2016, respectively. This study showed that the floods occurred in the end of melt season.

References

- Howat, I. M., A. Negrete, and B. E. Smith (2014), The Greenland Ice Mapping Project (GIMP) land classification and surface elevation data sets, *Cryosphere*, **8**, 1509–1518.
- Niwano, M., T. Aoki, K. Kuchiki, M. Hosaka, and Y. Kodama (2012), Snow Metamorphism and Albedo Process (SMAP) model for climate studies: Model validation using meteorological and snow impurity data measured at Sapporo, Japan, *J. Geophys. Res.*, **117**, F03008.
- Niwano, M., T. Aoki, K. Kuchiki, M. Hosaka, Y. Kodama, S. Yamaguchi, H. Motoyoshi, and Y. Iwata (2014), Evaluation of updated physical snowpack model SMAP, *Bull. Glaciol. Res.*, **32**, 65–78.
- Noël, B., W. J. van de Berg, E. van Meijgaard, P. Kuipers Munneke, R. S. W. van de Wal, and M. R. van den Broeke (2015), Evaluation of the updated regional climate model RACMO2.3: Summer snowfall impact on the Greenland Ice Sheet, *Cryosphere*, **9**(5), 1831–1844.

Keywords: Greenland, Glacier, Surface mass balance model, Flood

Validation of soil moisture contribution to near surface temperature by numerical sensitivity experiment in Northeastern Asia

*Enkhbat Erdenebat¹

1. Hokkaido University

Variations of near surface temperature of June-August due to difference soil moisture (SM) product is investigated by numerical experiments utilizing WRF model in Northeastern Asia. A 30-year (1981-2010) numerical experiment has conducted using ERA-interim reanalysis data as an initial and boundary condition to clarify the importance of SM contribution to the JJA extreme temperature and heat wave (HW). SM is known to be an important parameter to influence temperature by regulating surface energy balance through latent and sensible heat fluxes. To evaluate SM contribution to JJA temperature under similar atmospheric circulation, two experiments, reanalysis-SM (R-SM) as a control and satellite-SM (S-SM), have been compared. Both experiments were conducted during 20th May through 1st September. The S-SM experiment used initial SM condition derived from European Space Agency-Climate Change Initiative (ESA-CCI) dataset. During the numerical integration, SM can evolve as a result of atmosphere-land interaction. The model experiment has successfully generated the increasing trend of HW for frequency and intensity in R-SM. The result shows that S-SM experiments have improved the maximum surface air temperature and HW by 1.1°C and 0.7 days year⁻¹ on average during 1981-2010 in Mongolia. The amount of rainfall is reduced due to using S-SM as an initial condition in comparison to R-SM. In addition to rainfall, enhanced interaction of land and atmosphere is simulated in S-SM run, which higher positive anomaly at 500 hPa has developed in S-SM than R-SM by major HWs. Therefore sensitivity experiments confirm that ERA-interim estimates more SM in Northeastern Asia which results underestimate temperature and overestimates rainfall by model.

Time-lag effects of forest ecosystem response to climate change in continental dry climate zones over the circum-Arctic; a multiple approach using satellite images and tree-rings analyses

*Shunsuke Tei¹, Atsuko Sugimoto¹, Trofim Maximov^{2,3}

1. Arctic Research Center, Hokkaido University, 2. Institute for Biological Problems of Cryolithozone SB RAS, 3. BEST center, North Eastern Federal University

Circumboreal forest ecosystems are exposed to a larger magnitude of warming in comparison with the global average, as a result of warming-induced environmental changes. Understanding the sensitivity of tree growth to climate in these ecosystems is an important factor in the accuracy of future projections of the terrestrial carbon cycle, and also of global climate. However, it is not certain how these ecosystems respond to these changes.

In this study, we compared past 30 years spatio-temporal variation of Global Inventory Modeling and Mapping Studies (GIMMS) satellite derived normalized difference vegetation index NDVIg, its recent successor version NDVI3g, and tree-ring width index (RWI) on International Tree-Ring Data Bank (ITRDB) over circum-arctic region (>50N) with respect to relationship with climate change. The comparisons are conducted for linking those indices each other and for obtaining better estimate of vegetation activity response to climate change.

We calculate correlation coefficients between those indices and both previous and current year meteorological data, for each grid/site, and higher correlation coefficients were considered as actual response of forest ecosystem. Given the time lag effects of RWI or NDVI response to climate change, above indices in continental dry regions such as inner Alaska and Canada, southern part of Europe and southern sections of the Lena river basin in eastern Siberia tend to show significant negative correlation with summer temperature of previous year, suggesting further reduction of ecosystem carbon uptake with future warming.

Our findings highlight that the time lag effects of forest ecosystem response to climate change significantly affects relationships between both NDVI and RWI, and climate variables and it therefore should be incorporated into future carbon cycle studies. Otherwise, future projection of forest ecosystem carbon uptake may be overestimated under expected future further warming.

Keywords: Arctic and sub-Arctic ecosystems, carbon cycle, tree ring, remote sensing

The role of vegetation change upon polar amplification in warm climate by feedback analysis

*Ryouta O'ishi¹, Masakazu Yoshimori², Ayako Abe-Ouchi^{1,3}

1. Atmosphere and Ocean Research Institute, the University of Tokyo, 2. Hokkaido University, 3. JAMSTEC

Previous studies revealed that vegetation change in high latitude (e.g. from tundra to forest) in warm climate strengthens a polar amplification. This is due to lower vegetation albedo of forest than tundra, snow-albedo feedback caused by early snow melt due to forest coverage and ocean heat emission in autumn and winter. In the present study, we run a vegetation-coupled general circulation model with a slab-ocean, MIROC-LPJ, for two kinds of warming experiments. One is due to higher atmospheric CO₂ concentration (2xCO₂ and 4xCO₂) and the other is due to the difference of the Earth's orbit (mid-Holocene and the Last Interglacial). The result shows different mechanisms of warming amplification between CO₂-induced vegetation feedback and orbit-induced vegetation feedback. We also try to apply a feedback analysis (Cai and Luo 2009; Yoshimori et al. 2014) to the result of MIROC-LPJ experiments.

Keywords: polar amplification, vegetation, paleoclimate

Projecting future greenhouse gas release by global land surface-vegetation coupled model with explicit permafrost dynamics

*Tokuta Yokohata¹, Kazuyuki Saito², Hiroshi Ohno³, Go Iwahana⁴, Akihiko Ito¹, Kumiko TAKATA¹

1. National Institute for Environmental Studies, 2. Japan Agency for Marine-Earth Science and Technology, 3. Kitami Institute for Technology, 4. University of Alaska Fairbanks

Permafrost is distributed widely over polar region. Polar region is sensitive to climate change owing to the feedback processes related and ice and snow. Increase in permafrost temperature and thickening of active layer of frozen ground (upper layer of permafrost where frozen ground thaws in summer and freezes again during the autumn) are already observed. In addition, large-scale and irreversible melting of ice-rich permafrost layers called “Yedoma” and their ground subsidence are also reported in various places. Permafrost contains large amounts of organic carbon that has not been decomposed since last ice age, and thus melting of permafrost cause increase in the atmospheric greenhouse gases and possibly contribute to positive feedback to global warming. However, considerable uncertainty remains in the possible effects of permafrost melting on future climate change because global distribution of permafrost and details in the processes of GHG release from the permafrost are not known well. In the three-year project “Assessing and projecting greenhouse gas release from dynamic permafrost degradation” (2-1605, Environment Research and Technology Development Fund of the Ministry of the Environment, Japan: 2016-2018), we aims to assess and project the impacts of greenhouse gas release through dynamic permafrost degradation through in-situ and remote (e.g., satellite and airborne) observations, lab analysis of sampled ice and soil cores, and numerical modeling, by demonstrating the vulnerability distribution and relative impacts between large-scale degradation and such dynamic degradation. In this presentation, we report the status of the numerical modeling. We use a global physical land surface model MATSIRO (Takata et al. 2003, Nitta et al. 2014), which is a component of global climate model MIROC (Watanabe et al. 2010). In addition, a global land vegetation model VISIT (Ito et al. 2012) is coupled to MATSIRO and exchange variables such as soil moisture, temperature, and leaf area index with each other. We improved the physical processes related to permafrost melting (e.g., increasing in numbers in vertical layers; considering of changes in thermal conductivity of frozen/unfrozen soil water, and shielding effect by soil organic layer) in MATSIRO and found that seasonal distributions of permafrost tend to be improved. We also try to implement the carbon dioxide and methane release due to permafrost melting in VISIT to estimate the future greenhouse gas emission.

Keywords: Permafrost, Greenhouse gas, Climate change

Estimation of the Siberian fire in September 2016 on the concentration of ozone and BC in the Pan-Arctic region using a regional chemical transport model

*Masayuki Takigawa¹, Fumikazu Taketani¹, Yugo Kanaya¹, Takuma Miyakawa¹, Petr Mordovskoi¹, Masahiro Yamaguchi¹

1. Japan Agency for Marine-Earth Science and Technology

Black carbon (BC) particles strongly absorb sunlight, and it has recently emerged as a major contributor to the global climate change, possible second to CO₂ and methane. BC is produced both naturally and by human activities as a result of the incomplete combustion of fossil fuels, biofuels, and biomass. It is also known as a component of PM_{2.5}, and influences on the human health. BC also changes the Earth's albedo by changing the color of ice and snow via deposition into the surface, and the impact of BC on the climate change seems to be larger at polar region than that at the rest of the world. To estimate the impact of biomass burning on the concentration of BC and other pollutants, we had conducted model simulations over the Pan-Arctic region using a regional chemical transport model (WRF-Chem version 3.8.1). The initial and lateral boundary conditions for the meteorology were taken from NCEP-GFS. RACM and GOCART modules were used for the gaseous and aerosol chemistry, respectively. Anthropogenic emissions were based on EDGAR 4.2, and the biomass burning were based on the near-real-time version of FINN for each day. A pyro-convection process was also considered for the estimation of vertical profiles of biomass burning emissions. In the aerosol module of the model, BC particles were assumed to be emitted as hydrophobic BC, and were converted into hydrophilic BC by the folding time of 2.5 days. Biogenic emissions of VOCs were estimated by MEGAN 2.1 which is included in the model to use the meteorology and radiation calculated in the model for each time step. 50-days calculation with 15-days spinup was conducted from August to October 2016, when the Siberian forest fire were estimated to be quite active in the NCAR FINN inventory. To estimate the impact of biomass burning, we have conducted two calculations; 1) full emissions (anthropogenic, biogenic, and biomass burning) and 2) without biomass burning emissions (anthropogenic and biogenic). Meteorological field was compared with the observational data from the ship-based observation on R/V Mirai at the Arctic Ocean and Bering Sea, and model succeeded to reproduce the general variations of meteorological field such as the passage of low pressure systems. BC concentration at the surface level was increased over the Bering Sea after 25 September, and the main cause of the increase was estimated to be the biomass burning at around the Lake Baikal in late September. Biomass burning emissions of NO_x and VOCs also increased the concentration of ozone around the source region, and it reaches 40 ppbv as the maximum.

Keywords: Black Carbon, regional chemical transport model, Pan-Arctic, biomass burning

Weather Conditions During Large-Scale Widespread Forest Fires in Siberia: Conditions in Southern Sakha

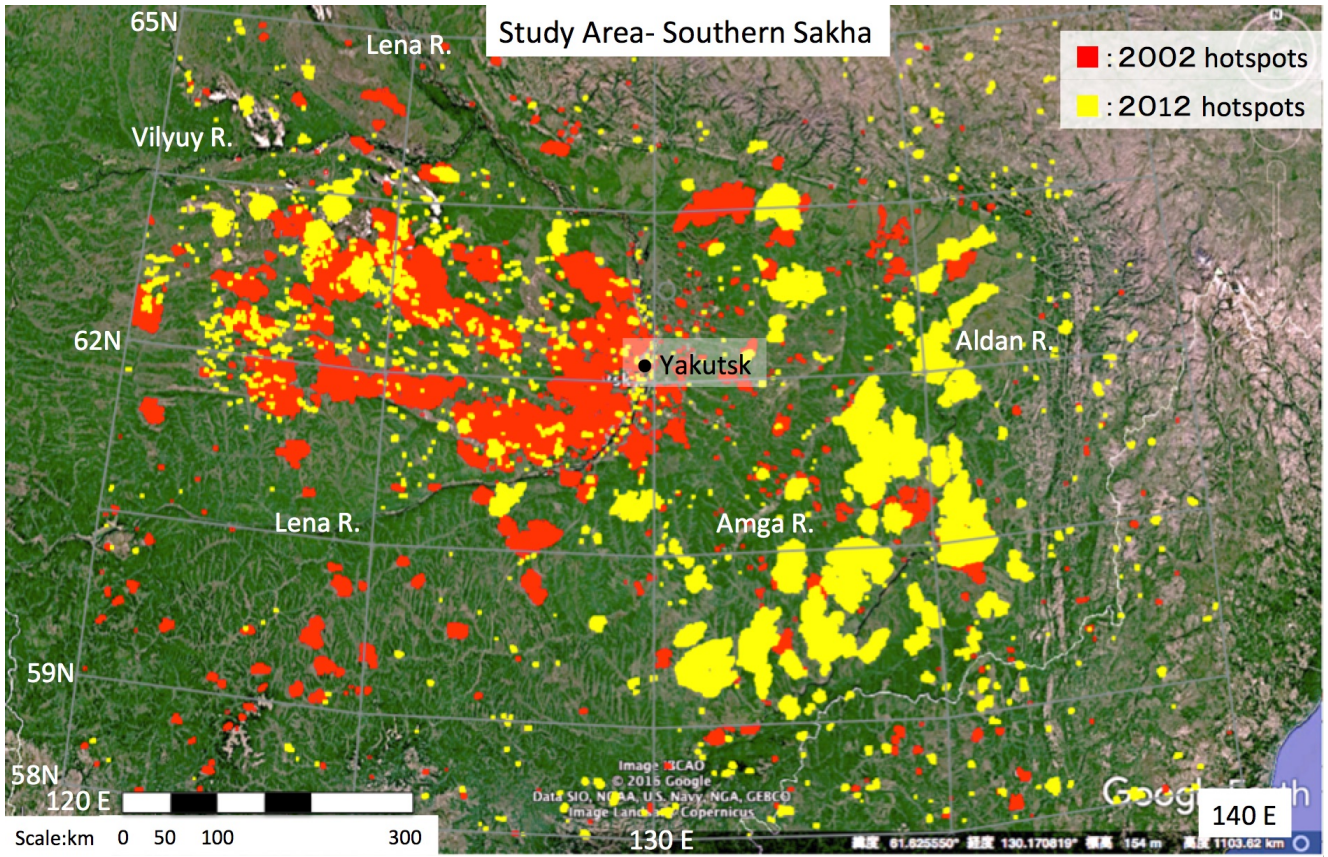
*Hiroshi Hayasaka¹

1. NPO Hokkaido Institute of Hydro-climate

In this vast Russian boreal forest, forest fires occur every year in various places. By analyzing Moderate Resolution Imaging Spectroradiometer (MODIS) hotspot data for more than 10 years, frequent fire regions in the Russian Forest are gradually becoming evident. In this report, we show the results of analyzing weather conditions of large forest fires in the boreal forest of Southern Sakha.

Large-scale forest fires depend on weather conditions after the occurrence of a fire. The authors have already clarified and reported synoptic scale weather conditions for recent large-scale fires in Alaska by analyzing MODIS hotspot data from 2003 to 2015. In Alaska, the top four fire periods occurred under similar unique high-pressure fire weather conditions related to Rossby wave breaking (RWB). Following the ignition of wildfires, fire weather conditions related to RWB events typically result in two hotspot peaks occurring before and after high-pressure systems move from south to north across Alaska. A ridge in the Gulf of Alaska resulted in southwesterly wind during the first hotspot peak. After the high-pressure system moved north under RWB conditions, the Beaufort Sea High developed and resulted in relatively strong easterly wind in Interior Alaska and a second (largest) hotspot peak during each fire period. In addition to these weather conditions, low-pressure-related fire weather conditions occurring under cyclogenesis in the Arctic also resulted in high fire activity under southwesterly wind with a single large hotspot peak. In boreal forest of Southern Sakha, large-scale forest fires occurred in 2002 and 2012. As a result of examining the weather conditions of four hotspot peaks in July and August of both years, two patterns of high-pressure and low pressure were also confirmed like in Alaska. In the high-pressure type, ridge was formed north of Yakutsk. In the low-pressure type, it became clear that low-pressure system in the Arctic Ocean played important role.

Keywords: Widespread fires, MODIS hotspot, Jet stream meandering



Interannual variability of summer precipitation over northern Eurasia in multiple climate models

*Manabu Abe¹, Hatsuki Fujinami², Tetsuya Hiyama²

1. Japan Agency for Marine-Earth Science and Technology, 2. Institute for Space-Earth Environmental Research, Nagoya Univ.

Global warming is projected to be amplified in high-latitude region. Because the Arctic sea ice loss has been already beginning to appear, hydrological cycle in the northern part of Eurasia may be affected by the global warming and the Arctic sea ice reduction. Fujinami et al. (2016) showed summer precipitation increased after 1980 in northern Eurasia, and Hiyama et al. (2016) discussed a possible effect of the recent Arctic sea ice reduction on the modulation of interannual variability of summer precipitation. Such changes are important issues for the current environment including the ecosystem over northern Eurasia. In addition, the reliable future projection and understanding of the hydrological cycle system are also important for mitigation and adaptation of future environmental changes.

In this study, we investigated characteristics of interannual variability of summer precipitation in northern Eurasia in 16 climate/earth system models, which have been used for the projection of future climate change, to assess whether recent global warming and the Arctic sea ice reduction affect realistically the northern Eurasian environment in the models. To reduce uncertainty related to oceanic change, we used data of the historical simulations of CMIP5 from 1979 to 2008 with observed sea surface temperature (SST) and sea ice conditions.

The spatial distribution of precipitation averaged for summer (June-July-August) in northern Eurasia in each model is similar to the observed one. Unlike the observed increase in summer precipitation in Siberian region (Fujinami et al. 2016), there is no model showing a remarkable increase trend of summer precipitation averaged over Siberian region. EOF analysis was performed for each model to extract the leading modes of interannual variability of summer precipitation in northern Eurasia. Although the EOF spatial patterns differs among the models, the first three EOF patterns of many models includes a pattern similar to the east-west seesaw pattern, which is a leading mode of the observed interannual variability. Furthermore, Hiyama et al. (2016) showed difference in the interannual variation pattern of observed summer precipitation in the northern Eurasia between the two periods before and after 1990, and also discussed the relationship between this difference and the Arctic sea ice reduction. Then we compared the frequency of EOF score values between the first 10 years (1979-1988) and the last 10 years (1999-2008) in each model. In many models, the mean or variance of score values at an EOF mode changed significantly between the periods. However, the spatial pattern of the EOF where the frequency change of the score value occurred was not similar between models.

As a result, the characteristics of interannual variability in northern Eurasia differ greatly among the models. However, it turned out that the observed east-west seesaw mode was included as one of the interannual variability in almost all of the models. In addition, some models revealed that the interannual variability of summer precipitation in northern Eurasia modulated after 1980, as discussed in Hiyama et al. (2016). In this presentation, atmospheric circulations related to the EOF modes are also shown.

References

Fujinami, H., Yasunari, T. and Watanabe, T. (2016), Trend and interannual variation in summer precipitation in eastern Siberia in recent decades. *Int. J. Climatol.*, 36: 355–368. doi:10.1002/joc.4352
Hiyama, T., H. Fujinami, H. Kanamori, T. Ishige, and K. Oshima (2016), Recent interdecadal changes in the interannual variability of precipitation and atmospheric circulation over northern Eurasia, *Environmental*

Research Letters, 11(6), 065001, doi:10.1088/1748-9326/11/6/065001.

Keywords: Interannual variability of summer precipitation, northern Eurasia, global warming

How Predictable Summer Arctic Cyclones in 2012 and 2016 Were?

*Akio Yamagami¹, Mio Matsueda^{1,2}, Hiroshi Tanaka¹

1. Center for Computational Sciences, University of Tsukuba, 2. Department of Physics, University of Oxford

Arctic cyclones (ACs) have a long lifetime and a wandering track in the Arctic region. The structures of the ACs are characterized by the warm and cold cores at upper and lower levels, downward and upward drifts at upper and lower levels, and barotropic relative vorticity. ACs have large impacts on the Arctic systems like the sea water temperature and the sea ice. ACs also have social impacts on the Northern Sea Route of ships and the Polar Route for airplanes. Therefore, accurate predictions of ACs are important for environmental and social concerns.

Extreme ACs occurred in August 2012 and 2016. The AC in 2012 (AC2012) was generated over the north of the Eurasia on 2 August 2012. The minimum sea level pressure (SLP) of 964 hPa for the AC2012 was recorded on 6 August 2012. On the other hand, the cyclogenesis of the AC in 2016 (AC2016) was over the north of the Scandinavian Peninsula on 11 August 2016. The minimum SLP of 967 hPa for the AC2016 was recorded on 16 August 2016. Although the positions of the cyclogenesis were different, both ACs recorded the minimum SLP over the Pacific sector of the Arctic Ocean. In both cases, the AC merged with a cyclone connecting with an upper polar vortex over the Arctic Ocean few days before the development of the AC. Some previous studies indicated that the AC2012 contributed greatly to the record low sea-ice extent in that summer. Similarly, it is thought that the AC2016 could have an influence on the decrease in sea-ice cover, since sea ice extent in early September of that year was the second lowest on record.

In this study, we investigated the predictability of the extreme ACs in August 2012 and 2016, using operational medium-range ensemble forecasts provided by The Interactive Grand Global Ensemble (TIGGE). The minimum SLP of the AC2012 on 6 August was well predicted by CMC, ECMWF, and JMA (NCEP and UKMO) members 2 (3) days in advance. Some ECMWF and NCEP members initialized in late July 2012 also predicted the development of the AC2012. On the other hand, the minimum SLP of the AC2016 was more predictable than that of the AC2012. The development of the AC2016 was well predicted by ECMWF members 6 days in advance and by CMC, JMA, NCEP and UKMO 3 –5 days in advance. Comparisons between higher- and lower-skill members revealed that the accurate prediction for the development of the upper warm core could lead to the accurate prediction of the AC development in both cases. Baroclinic growth and subsequent nonlinear dynamics during the merging contributed to the development of the upper warm core. Even if the baroclinic growth was predicted well, predicted AC did not develop when the merging was not predicted accurately. Therefore, a correct prediction of for the AC track is one of the important factors for accurate prediction of the AC development. The predicted cyclone track was similar to the observed cyclone track when the upper-level wind was predicted well. In conclusion, the accurate prediction of the upper-level wind can lead to the correct prediction of the ACs through the development of the upper warm core.

Keywords: Arctic cyclone, warm core, cyclone merging, ensemble forecast

Influence of Springtime Eurasian Snow Cover Retreat on Atmospheric Circulation over East Asia

*Toru Nozawa¹, Subaru Fujiwara¹

1. Graduate School of Natural Science and Technology, Okayama University

According to the 5th Assessment Report of the Intergovernmental Panel on Climate Change, springtime snow cover extent over the Northern Hemisphere (NH) is greatly retreating since 1990's. Recent study also pointed out that vanishing cryosphere may affect extreme summer weather in NH mid-latitudes. In this study, we investigate impacts of springtime Siberian snow cover fraction (SCF) change on atmospheric circulations in Northern mid-latitudes, especially over the East Asia, using a new satellite-observed SCF product by JAXA and the Japanese 55-year Reanalysis dataset.

Composite analysis suggests that, when the SCF over Western Siberia is significantly low in April, upper and middle tropospheric jet stream over Japan shifts southward in April and the following June. Land surface temperature significantly increases and soil moisture significantly decreases over southern part of Western Siberia and Central Asia in June. In addition, sensible heat flux from the surface to the atmosphere significantly increases in May and June, and significantly warms the atmosphere over there. These results suggest that the reduction of snow melted water suppresses evaporation of soil moisture when snow vanished, and causes warmings of the land surface, increases in the sensible heat flux, and warmings of the middle and upper air, which may affect the atmospheric circulation changes.

Keywords: Global warming, Snow cover, Land and atmosphere interaction

Variation of recent annual snow depositions estimated on the 2016 pit observation at the East Greenland Ice Core Project (EGRIP) camp

Fumio Nakazawa^{1,2}, *Naoko Nagatsuka¹, Kumiko Goto-Azuma^{1,2}, Dorthe Dahl-Jensen³, Jørgen Peder Steffensen³

1. National Institute of Polar Research, 2. SOKENDAI (The Graduate University of Advanced Studies), 3. Niels Bohr Institute, University of Copenhagen

East Greenland Ice Core Project (EGRIP), which is an international ice coring project led by University of Copenhagen in Denmark, commenced in 2015 to clarify the variations of climate and ice sheet in Greenland. We are participating in the project under the Arctic Challenge for Sustainability project (ArCS), and cooperative research is underway with various countries. We dug two pits with depths of 4.02 and 3.18 m at the EGRIP camp (75°37'N, 35°59'W) to estimate recent annual and seasonal snow depositions and concentrations of chemical species and dust particles in the snow samples. Snow sampling and snow density measurement were carried out at 0.03 m interval in those pits. Currently, measurements of the water stable isotope ($\delta^{18}\text{O}$ and δD) for the 4.02-m deep pit have been completed. Clear seasonal variations in the stable isotopes of water were observed in the depth profiles, which suggested that snow had accumulated regularly every year. Also, the seasonal cycles of $\delta^{18}\text{O}$ and δD showed the pit included snow deposition corresponding to nine years covering 2008–2016. The annual snow depositions ranged from 99 to 247 mm water equivalent (w.e.), showing the mean value of 167 mm w.e. The pit observation of 2 m deep conducted at North Greenland Eemian Ice Drilling (NEEM) camp in northern Greenland reported that the mean annual snow deposition was 176 mm w.e. during the years 2006–2008, and the value was on the same level with that at the EGRIP. The profile of snow density in the pit indicated a seasonal variation, in which the density increased in the winter layers and decreased in the summer layers. The same trends were also found at NEEM and Summit in Greenland in the previous studies (Albert and Shultz, 2002; Kuramoto et al., 2011). A wind-pack effect in winter may cause the higher density observed at EGRIP, as discussed in the previous studies. We will also show analyses of the chemical species and dust particles for the 4.02-m deep pit and results of the 3.18-m deep pit on the presentation.

Keywords: Greenland, ice core, mass balance, snowpack, stable isotope ratio

Seasonal variations of Greenland ice sheet surface reflectance and brightness temperature derived from Terra/MODIS and GCOM-W/AMSR-2

*Rigen Shimada^{1,2}, Masahiro Hori¹, Nozomu Takeuchi³, Teruo Aoki^{2,4}

1. Japan Aerospace Exploration Agency, 2. Meteorological Research Institute, 3. Chiba University, 4. Okayama University

Dark ice area expansion on the Greenland ice sheet is one of the factors to cause albedo reduction and mass loss of the ice sheet in recent years. Dark ice appears on ablation area in summer and accelerates melting of the ice sheet due to its intense light absorption. Dark ice is due to impurities in the surface ice such as mineral particles, glacial microbes, organic matter and their aggregate called cryoconite granules. Cryoconite granules are formed by microbial activities and are darker than abiotic mineral particles. Since the microbes can be active only on melting ice surface, duration of surface melting on the ice sheet possibly affect the microbial activities and thus formation of cryoconite granules. Therefore, spatio-temporal variation in surface melting is important to understand the darkening process. We report seasonal variations in surface reflectance and brightness temperature derived from Terra/MODIS and GCOM-W/AMSR-2 satellite images in order to understand relationship between darkening and surface melting processes of the ice surface from April to August in 2013, 2014, 2015 and 2016. Reflectance (660 nm) and brightness temperature (18 GHz Horizontal polarization) were investigated at the nearest neighbor pixel of the Automatic Weather Station (67.07N, 48.83W) installed by PROMICE. The brightness temperature showed similar timing of the onset of surface melting in 2013 and 2015. In these years, the melting onset occurred in early June. On the other hand, the melting onset occurred in mid May in 2014 and 2016. The surface reflectance started to decrease down to around 0.4 in mid July 2013 and early July 2015. In contrast, it rapidly decreased down to around 0.4 in the end of June 2014 and early June 2016. These results suggested that earlier onset and prolonged period of the surface melting causes the earlier appearance of the dark ice surface.

Keywords: Greenland ice sheet, satellite remote sensing, dark ice

Long-term variability in land snow cover, sea ice extent and ocean color in Arctic region

*Shun Tsutaki¹, Masahiro Hori¹, Hiroshi Murakami¹

1. Japan Aerospace Exploration Agency

Satellite-based observations revealed that sea ice extent and land snow cover in the Arctic region have decreased since 1979 under the influence of warming trend. Reduced sea ice cover increases open water area, a longer growing season, and annual net primary production (NPP) by phytoplankton. The greatest contribution to the Arctic Ocean's freshwater input is the discharge from terrestrial rivers. Because river inflow supplies a large amount of nutrient salts and organic matter to the ocean, change in the discharge affects the Arctic Ocean's NPP. Thus, successive observations on sea ice extent and land snow cover are crucial to understand the influence of those area reductions on marine ecosystems in Arctic region. In this study, we used multiple optical and microwave radiometric satellite data for 1978–2015 to analyze land snow cover, sea ice extent and ocean color in the northern hemisphere. Sea ice extent decreased during the observation period with the mean rate of $200 \text{ km}^2 \text{ a}^{-1}$. Snow cover extent decreased in all seasons (winter, spring, summer and autumn) from 1978 to 2015. Decreases in land snow cover and sea ice extent are likely to affect to seasonal and inter-annual variabilities in the amount of freshwater inflow to the Arctic Ocean. However, no clear trend of the ocean color (chlorophyll-a concentration) was observed with statistically significant in this study. To better understand relationship between spatiotemporal variabilities in these factors and other physical parameters, we also analyze variability in sea surface temperature and meteorological parameters and examine their cross-correlation relationship in space and time.

Effect of subglacial meltwater plume formation on phytoplankton growth in the fjord of Bowdoin Glacier in northwest Greenland

*NAOYA KANNA¹, Shin Sugiyama^{1,2}, Yoshihiko Ohashi^{2,3}, Daiki Sakakibara¹, Bungo NISHIZAWA⁴, Izumi ASAJI^{2,3}, Yasushi FUKAMACHI^{1,2}

1. Arctic Research Center, Hokkaido University, 2. Institute of Low Temperature Science, Hokkaido University, 3. Graduate School of Environmental Science, Hokkaido University, 4. Faculty of Fisheries Sciences, Hokkaido University

In Greenland, marine-terminating outlet glaciers discharge turbid subglacial meltwater into fjords. The area influenced by the turbid water near the calving front is well known as an important foraging hotspot for higher trophic animals. Glaciers may therefore play an important role in ecosystem productivity within the fjords by releasing an essential macronutrient for primary producers. However, since there are few available data on the macronutrient delivery with the meltwater inputs, processes of macronutrient supply to surface waters are poorly understood. Here we present a hydrographic and geochemical dataset from Bowdoin Glacier and its fjord in northwestern Greenland during the summer of 2016.

On the glacier, meltwater contained few macronutrients ($<0.5 \mu\text{M NO}_3+\text{NO}_2$) indicating that supraglacial meltwater is not a significant source of macronutrients in the fjord. At the surface of a meltwater plume near the calving front, water properties were largely different from surface waters outside of the plume. The concentration of surface macronutrients inside the plume was an order of magnitude higher ($\sim 12.8 \mu\text{M NO}_3+\text{NO}_2$) than that outside of the plume ($<1.6 \mu\text{M NO}_3+\text{NO}_2$). Additionally, salinity (~ 33.0) and the content of suspended particles ($\sim 132 \text{ mg/L}$) inside the plume were notably higher than those outside of the plume (salinity ~ 15.4 ; suspended particles $\sim 22.3 \text{ mg/L}$), suggesting upwelling of nutrient-rich, saline deep water including substantial sediment derived from subglacial weathering. Oxygen isotopic compositions of the glacial meltwater, plume, and fjord water also indicated that the glacial meltwater upwells as a buoyant flow, drawing the nutrient-rich deep water into the fjord. Within a vertical cross-section along the centerline of the fjord, highly turbid water was observed in sub-surface layer at depths of 10–50 m. Less saline water with low macronutrients concentration was on top of this highly turbid water. Phytoplankton blooms ($\sim 6.5 \mu\text{g/L}$ chlorophyll a) was observed near the boundary between the less saline water and the turbid water. The concentration of macronutrients was sufficiently high ($\sim 10 \mu\text{M NO}_3+\text{NO}_2$) in this area to generate the bloom. Overall, our study results show that turbid meltwater discharge from Bowdoin Glacier affects nutrient availability and the subsequent growth of phytoplankton in the fjord. Upwelling and transport of macronutrients associated with subglacial meltwater plume formation is an important process for phytoplankton growth in the near-surface layer.

Keywords: Greenland, Bowdoin Glacier, Macronutrient, Turbid meltwater discharge

Fe, Mn, Cd, and Pb Quantitatively Analysed in Sea Ice

*La Kenya Evans^{1,3}, NAOYA KANNA², Jun Nishioka³

1. Graduate School of Environmental Sciences, Hokkaido University, 2. Arctic Research Center, Hokkaido University, 3. Institute of Low Temperature Sciences, Hokkaido University

Sea ice plays a significant role in polar oceans. During sea ice formation both dissolved and particulate sea water constituents (trace metals, macro-nutrients, sediments, etc) accumulate through scavenging or suspension freezing (Reimnitz et al., 1992,1993; Nürnberg et al., 1994). This can allow for sea ice to hold trace metal concentrations higher than the underlying water (Grotti et al. 2005; Tovar-Sanchez et al. 2010). Floating (pack) sea ice can then transport incorporated materials into new areas as it melts, seeding the water community below (van der Merwe et al., 2011). Although many studies have looked at sea ice and trace metals, the mechanism and geochemical cycling role for trace metal accumulation is still largely unknown (Kanna et al., 2014). In this study we examined the following metal fractions for Fe, Mn, Cd and Pb: Dissolved (D, $<0.2 \mu\text{m}$), and Labile Particulate (LP, Total Dissolvable - Dissolved) from Chukchi Sea pack ice and the surrounding seawater (shelf and coast). Samples were pre-concentrated utilizing the solid-phase extraction NOBIAS Chelate PA1 resin (Hitachi High-Technologies) following a modification of Sohrin et al. (2008) and Kondo et al. (2016) methods. Finally, samples were analyzed on a Graphite Furnace Atomic Absorption Spectrometer (GFAAS). Applying the modified solid-phase extraction method on sea ice measurements allowed us to accurately detect low levels of trace metals. Utilizing this method allowed us to gain insightful information on the geochemical cycling of trace metals within sea ice.

LPF_e, LPM_n and LPP_b composed 98-99% of Fe, Mn and Pb in Chukchi sea ice where LPC_d was 84%. Although Cd and Pb were detectable, the concentrations for the dissolved and labile particulate fractions were very low ($0.05 \pm 0.04 \text{ nM}$ – $6.3 \pm 5.9 \text{ nM}$). Overall in sea ice and seawater, the labial particulate fraction had higher concentrations than the dissolved. Sea ice has been shown to have a temporal decoupling of trace metals (i.e. Fe), with the dissolved metals being released with the brine and particulate metals release with advanced melting (van der Merwe et al., 2011). Since our samples were collected during summer, advanced melting could have led to the dominance of the labile particulate fraction. Chukchi seawater (shelf and coast) samples also showed the same trends where Fe and Mn had higher concentrations than Cd and Pb. LPF_e and LPP_b composed 99-100% of Fe and Pb in Chukchi seawater. One interesting point was that Pb was detectable in sea ice for both the dissolved and labile particulate fractions but only detectable as LPP_b in seawater. Mn and Cd composition in Chukchi seawater was dominated by the dissolved fraction (75% and 43% respectively). DFe is removed from seawater by oxyhydroxide formation and particle scavenging, which can give it have lower concentrations than DMn (Landing and Bruland, 1987).

Keywords: Sea Ice, Trace Metals, Dissolved, Labile Particulate

Distribution of the Anadyr Water near the Gulf of Anadyr and the Bering Strait

*Toru Hirawake¹, Issei Nakagawa², Jun Nishioka³

1. Faculty of Fisheries Sciences, Hokkaido University, 2. Graduate School of Environmental Science, Hokkaido University, 3. Institute of Low Temperature Science, Hokkaido University

Primary production in the Bering Strait (BS) especially in the Russian side is extremely high and it is found not only in spring but also in summer and autumn seasons. It has been suggested that the continuous high phytoplankton activity is attributed to rich amount of nutrients in the Anadyr Water (AW). Although some literatures reported higher nutrients concentration in the Gulf of Anadyr (GA), similar level of primary production as the BS is difficult to be observed in the GA. In this study, we obtained a historical CTD dataset (1930–2005) compiled at the Far Eastern Regional Hydrometeorological Research Institute (FERHRI) in Russia and investigated water mass structure from the GA to the BS. We analyzed the dataset climatologically because stations of each cruise distribute sparsely. In August, while the AW with high salinity (>35 PSU) distributed near the bottom of the GA, the Bering Shelf Water was covered the surface of the Gulf. The AW was spread along coast of Russia and a part of it was found in the surface of BS. The water mass structure in this study suggests that the AW from the AG continuously supports high primary production in summer of the BS.

Keywords: Gulf of Anadyr, Anadyr Water, Bering Strait

Interannual variability of bottom oxygen concentration and primary production in the southern Chukchi Sea biological hotspot

*Amane Fujiwara¹, Shigeto Nishino¹, Toru Hirawake², Takashi Kikuchi¹

1. Japan Agency for Marine-Earth Science and Technology, 2. Hokkaido University

Hope valley located in the southern Chukchi Sea is known as one of the biological hotspot (southern Chukchi Sea hotspot, SCH). Large benthic biomass in the SCH is supported by high primary productivity of the water column. The dissolved oxygen (DO) sharply decreases at the bottom toward fall as a result of the high sediment community oxygen consumption in the benthic fauna, while it is saturated during winter. We examined annual/inter-annual variability of bottom DO and its mechanisms analyzing ship-board and mooring hydrographic data, satellite derived primary production, and ecosystem model. The bottom DO showed large interannual variability (104–300 μM) and it was negatively and significantly correlated with cumulative primary production ($r = -0.66$, $p < 0.05$). Such negative correlation suggests organic carbon flux to the sea floor drives the activity of the benthic community. Environmental process of decreasing in DO was assessed using one box ecosystem model optimized for the SCH bottom layer. The model also captured bottom DO is sensitive to the flux of primary production from the upper layer. Our results suggest inter-annual variability of primary production is a key factor determining the recent changes in biomass and distribution of the benthic organisms.

Keywords: biological hotspot, primary production, bottom oxygen concentration

Annual monitoring on lateral advection of shelf materials off the Barrow Canyon, western Arctic Ocean

*Jonaotaro Onodera^{1,2}, Eiji Watanabe², Kohei Mizobata³, Yuichiro Tanaka⁴, Kazumasa Oguri⁵, Naomi Harada^{1,2}

1. Research and Development Center for Global Change, JAMSTEC, 2. Institute of Arctic Climate and Environment Research, JAMSTEC, 3. Tokyo University of Marine Science and Technology Department of Ocean Sciences, 4. The Research Institute of Geology and Geoinformation, AIST, 5. Department of Marine Biodiversity Research, JAMSTEC

Lateral transportation of heat and materials from shelf to basin is important keys to understand ecosystem and biogeochemical cycles in the southwestern Canada Basin. The physical oceanographic model suggested that the westward advection of oceanic eddies from off the Barrow Canyon contributed to the temporal increase of high settling particle flux at Station NAP in the southern Northwind Abyssal Plain (75° N 165°W). In order to monitor the shelf-basin interaction in upper stream area of Station NAP, annual bottom-tethered mooring with sediment trap and hydrographic sensors were deployed off the Barrow Canyon (Station NBC15t, 72.47°N 155.41°W) from October 2015 to September 2016. The trapped particles contained abundant lithogenic matters which were derived from continental shelf. Total mass flux at ~243 m depth where sediment trap was deployed at NBC15t ranged from 14.6 to 3413.9 mg m⁻² d⁻¹ before the trap clogged in June 2016. The maximum of total mass flux was one order higher than that at Station NAP. The maxima of total mass flux were observed in the periods of 5-18 October 2015 and 12-24 May 2016. In addition, the underwater camera mounted on sediment trap recorded an image with abundant particles in September 2016. The comparison with hydrographic sensor data and the video record of underwater camera suggests that shelf material component of trapped particles in October 2015 and September 2016 were supplied by intensified lateral water current in subsurface layer shallower than the deployment depth of sediment trap. The high particle flux in May 2016 is explained by intensified water current containing abundant particulate matters in limited subsurface layer between the ADCP (~125m depth) and sediment trap depths.

Keywords: Arctic Ocean, Canada Basin, Settling particle flux, Shelf-basin interaction

Impacts of terrestrial river heat flux on the declining Arctic sea ice

*Hotaek Park¹, Kazuhiro Oshima¹, Yasuhiro Yoshikawa², Eiji Watanabe¹

1. Japan Agency for Marine-Earth Science and Technology, 2. Kitami Institute of Technology

In the Arctic, the recent warming speed of surface air temperatures are the fastest among the past historical records. The consequent influences are found in changes in the Arctic freshwater system, such as increasing river discharge, changing river-ice phenology, and warming of river water temperature. The warming water temperature can result in higher heat flux flowing into the Arctic Ocean, combining with the larger river discharge, which likely enhances the melt of sea ice in the shelf area. However, very few studies quantitatively assessed influences of the river heat flux on the Arctic sea ice are available. A land surface model (CHANGE) coupled with models of river discharge, ice-cover, and water temperature through channel network was applied to the Arctic river basins over the period 1979–2013, and then we assessed influences of the river processes on sea ice, including trends of river discharge, water temperature, and heat flux. The simulation indicated obvious increases in river discharge and water temperatures over the pan-Arctic rivers, consequently flowing considerable amount of heat to the ocean. The heat fluxes were significantly correlated with changes of sea surface temperature and sea ice concentration in the coastal areas of the Arctic Ocean, especially in the spring season when the sea ice begins to melt. This emphasizes that the heat flux of terrestrial freshwater is an important factor influencing the melting process of sea ice at specifically seasonal and local scales.

Keywords: river heat flux, sea ice retreat, land surface mode, sea ice concentration

Interannual variation of solar heating in the Chukchi Sea, Arctic Ocean

*Yushiro Tsukada¹, Ueno Hiromichi¹, Naoki Ohta³, Motoyo Itoh², Eiji Watanabe², Takashi Kikuchi², Shigeto Nishino², Kouhei Mizobata⁴

1. Graduate School of Fisheries Sciences, Hokkaido University, 2. Japan Agency for Marine-Earth Science and Technology, 3. Graduate School of Environmental Science, Hokkaido University, 4. Graduate School of Marine Science and Technology, Tokyo University of Marine Science and Technology

Arctic sea ice cover in summer has declined rapidly over the past few decades. The albedo of sea ice is much higher than that of open water; reduction of sea ice cover is associated with increase of solar heating in the Arctic Ocean. In this study, we focus on solar heating in the Chukchi Sea located in the Pacific side of the Arctic Ocean where remarkable sea ice reduction has occurred. The Chukchi Sea is a pathway of Pacific Water from the Bering Strait to the Arctic Basin. The heat transport of the Pacific Water through the Bering Strait, which has increased recently, plays an important role in a decrease in sea-ice formation during winter as well as sea-ice melt in summer in the Canada Basin. Although the Pacific Water heat transport through the Bering Strait is becoming clearer, we expect that solar heating significantly modifies the Pacific Water in the Chukchi Sea. Therefore, we estimate solar heating in the Chukchi Sea through analysis of satellite-derived sea ice concentration data as well as reanalysis data of shortwave radiation, and discuss the role of the solar heating in the Chukchi Sea in the heat transport into the Arctic Basin. We also use in-situ shortwave radiation data obtained by R/V Mirai to validate the reanalysis data of shortwave radiation in the Chukchi Sea.

Keywords: Chukchi Sea, solar heating

Pacific water fluxes through the Barrow Canyon and its effect on warming in the Arctic Ocean

*Motoyo Itoh¹, Takashi Kikuchi¹, Shigeto Nishino¹

1. Japan Agency for Marine-Earth Science and Technology

Over the past few decades, sea ice retreat during summer has been enhanced in the Pacific sector of the Arctic Basin, in part due to increasing summertime heat flux of Pacific-origin water from the Bering Strait. Barrow Canyon, in the northeast Chukchi Sea, is a major conduit through which the Pacific-origin water enters the Arctic Basin. Our study focuses on the quantitative estimate of volume, heat and freshwater fluxes through Barrow Canyon by mooring observations and its role in warming of upper layers in the Canada Basin. We conducted year-round mooring observations from 2000 to 2016 in the mouth of Barrow Canyon. The annual mean poleward volume, freshwater and heat fluxes through Barrow Canyon were 0.43 Sv, 31 mSv and 2.12 TW. The annual averaged heat flux displayed substantial interannual variability, ranging from 0.93 TW to 3.34 TW. Comparing heat content in the Barrow Canyon and satellite derived sea surface temperature around Barrow Canyon, we derive and assess a proxy for estimating heat content in the canyon for the summer time period, which is when most of the heat passes northward towards the basin. The estimated heat content shows increasing trend from 1980 to 2015 and 1.5 times larger than the average value from 1980s to 2010s. Measurements from hydrographic surveys since 1990 reveals that warming of Pacific summer water layer in the Canada Basin tended to be enhanced around 2010s, probably due to higher heat transport via Barrow Canyon into the basin in 2007, 2010 and 2012.

Keywords: Arctic Ocean, Ocean warming, Sea ice reduction

Seasonal variability of near-inertial internal waves and its kinetic energy in the ice-diminishing Arctic Ocean

*Yusuke Kawaguchi¹, Motoyo Itoh¹, Takashi Kikuchi¹, Jonaotaro Onodera¹, Naomi Harada¹, Yasushi Fukamachi², Erika Moriya³

1. JAMSTEC Japan Agency for Marine-Earth Science and Technology, 2. Arctic Research Center, Hokkaido University, 3. Hydro System Development, Inc.

In the Arctic ocean, the internal wave activity and its contribution to the turbulent mixing has been considered to be quite low. In the modern era, the Arctic sea-ice extent has been dramatically diminishing, and therefore there is an increased chance of kinetic energy input from the air at ocean surface. In this study, the seasonal change of near-inertial internal wave (NIW) kinetic energy is examined in comparison with local sea ice compactness and draft thickness. The local sea-ice information was obtained using an ice profiling sonar mounted at top of a moored instrumentation in the Northwind Abyssal Plain. The band-passed kinetic energy was recorded with a moored ADCP for depths within upper 110 m. The data clearly documented that the depth-integrated NIW kinetic energy varied in line with the ice seasonality, i.e., ice thickness and mobility. During ice covered months, the upper water NIW kinetic energy was approximately 1/10 of the Garrett-Munk (GM) canonical level. In the meantime, during the ice absent months of September and October, the kinetic energy levels built up closer to the GM level. The fine-scale parameterization (Gregg, 1989) estimates the turbulent mixing dissipates the incident wave energy at a rate of $O(10^{-10} - 10^{-9} \text{ W kg}^{-1})$. According to a mixed layer slab model (Pollard & Millard 1970), the energy input from the ice movement was 1.6 kJ m^{-2} , in which 13% was presumably dissipated through the wave-wave interaction in the upper 110 m. The ice-water combined velocity data also indicated that the mobility of sea ice floes can affect the kinetic energy amount in the upper water, suggesting the occurrence of increased turbulent energy as more unconsolidated ice exists in the future.

Keywords: Arctic Ocean , Near-inertial internal wave, Sea ice retreat